PREDICTING THE HEAD-LEAKAGE SLOPE OF CRACKS IN PIPES SUBJECT TO ELASTIC DEFORMATIONS

AM Cassa, JE van Zyl

A.M. Cassa, Golder Associates Africa, P.O. Box 6001, Halfway House 1685, Gauteng, South Africa, Tel: +27 11 313 1122, Fax: +27 11 315 0317, ACassa@golder.co.za

J.E. van Zyl, University of Cape Town, Cape Town, South Africa, Tel: +27 21 650 2325, kobus.vanzyl@uct.ac.za

Abstract

Pressure has a major impact on the rate of leakage from leak openings in pipes and studies have shown that the leakage exponents in networks can be substantially larger than the theoretical orifice exponent of 0.5. The most important reason for this behaviour is that leak areas are not fixed, but increase as a function of pressure.

In this study Finite Element analysis was used to investigate the relationship between pressure head and leak area in pipes with longitudinal, spiral and circumferential cracks. It was found that there is a linear relationship between crack area and pressure head for all crack types, pipe materials and loading conditions tested. The impact of loading, material, section and crack properties on the head-area slope was also investigated, and an attempt was made to find an expression to express the head-area slope as a function of these properties. Mathematical relationships were developed that give reasonable descriptions of the head-area slopes of longitudinal, spiral and circumferential cracks. With these

relationships it will be possible to predict the behaviour of different types of leak openings in different pipes and pipe materials.

Keywords: Leakage; pressure; failures

INTRODUCTION

The conventionally used equation for leakage as a function of pressure is described by the equation:

$$Q = ch^{N1} \quad (1)$$

where Q is the flow rate in m^3/s, c is the leakage coefficient, h is the pressure head in m, and $N1$ is the leakage exponent. Studies conducted on the relationship between pressure and leakage in water distribution systems have shown that the rate of flow from a leak is greatly affected by the pressure and that the resulting leakage exponents can be substantially larger than the theoretical orifice exponent of 0.5 (Farley & Trow 2003). The main reason for this behaviour is that leak areas are not fixed, but increase with increasing pressure. This study investigated the relationship between pressure and the leak area in pipes with longitudinal, circumferential and spiral cracks using Finite Element Analysis. Only linear elastic material behaviour was considered. Sensitivity analyses were conducted to determine the effect the crack properties (orientation, length and width), pipe material properties (Young's modulus, Poisson's ratio and longitudinal stress) and pipe section properties (internal diameter and wall thickness) have on the behaviour of each crack. This led to the development of equations to predict the response of the different cracks to variations in pressure.

FINITE ELEMENT ANALYSIS

The Finite Element Method is an established numerical analysis technique used for obtaining approximate solutions to a wide variety of engineering problems. Finite elements are used by creating different geometric regions, establishing separate approximating functions in each region and then joining them together to make a model containing many small interconnected sub-regions of elements. This study first used finite elements to analyse the behaviour of longitudinal, spiral and circumferential cracks in pipes under pressure.

The ABAQUS Finite Element software was used in this investigation as well as the software program Solidworks where the pipes were modelled according to the dimensions required. The study is based on a 110 mm diameter class 6 uPVC pipe with a wall thickness of 3 mm. The dimensions and properties of the test pipe are given in Table 1.

Table 1 – Dimensions and properties of a class 6 uPVC pipe

	Variable	**Value**	**Units**
Material Properties	Pressure head, h	600	kPa
	Young's modulus, E	3	GPa
	Poisson's ratio, v	0.4	–
	Longitudinal stress, σ_l	5.2	MPa
Geometry of pipe	Length of pipe, L_{pipe}	900	mm
	Wall thickness, t	3	mm
	Internal Diameter, ID	104	mm
Crack geometry	Length of crack, L_{crack}	60	mm
	Width of crack, W_{crack}	1	mm

Ten-noded quadratic tetrahedron elements were used throughout the pipes. The use of this element increases the accuracy of the result, as the tetrahedron element is not only giving four values at each corner of the element, but it also calculates a centre node between the corner nodes resulting in ten nodes as shown in Figure 1. Sensitivity analyses were done for each configuration to determine the optimal element size. Generally the sizes of the elements in the region around the cracks were 1 mm and 2 mm for all three

types of cracks while the rest of the pipe had element sizes of 5 mm. An example of a mesh is shown in Figure 2 of a spiral crack.

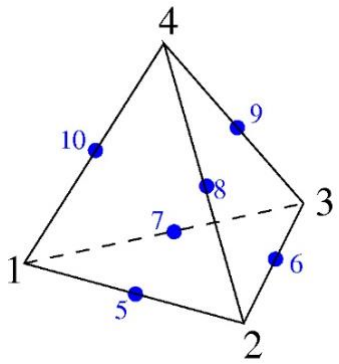

Figure 1 – Example of a quadratic tetrahedron element

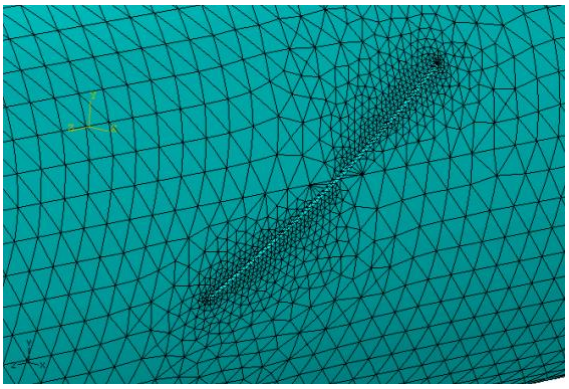
Figure 2 – A detailed look at the mesh around a spiral crack

The boundary conditions of the pipe consisted of clamping the pipe along an internal line on the opposite side of the crack and along the whole length of the pipe, as well as a point on the outside of the pipe adjacent to the internal line. The pipes were loaded with a uniform internal load to simulate water pressure, and a external stresses at the pipe ends to simulate the longitudinal pipe stresses. The pipe was assumed to lie in a horizontal plane. In the biaxial load state, the longitudinal pipe stresses were calculated using Equation (2) for longitudinal stress for cylindrical pressure vessels (Gere, 2001).

$$\sigma = \frac{Pr}{2t} \tag{2}$$

where *r* is the inner radius of the pipe, *P* the internal pressure, *t* the thickness of the pipe wall and σ the longitudinal stress. In the uniaxial load state, longitudinal stresses were assumed to be zero.

The three cracks were modelled with a constant radial tip edge corresponding to the width of the crack. Figure 3a shows the stress distribution around a longitudinal crack at a pressure of 600 kPa. The same crack is shown in Figure 3b using a deformed scale to show deformation in more detail.

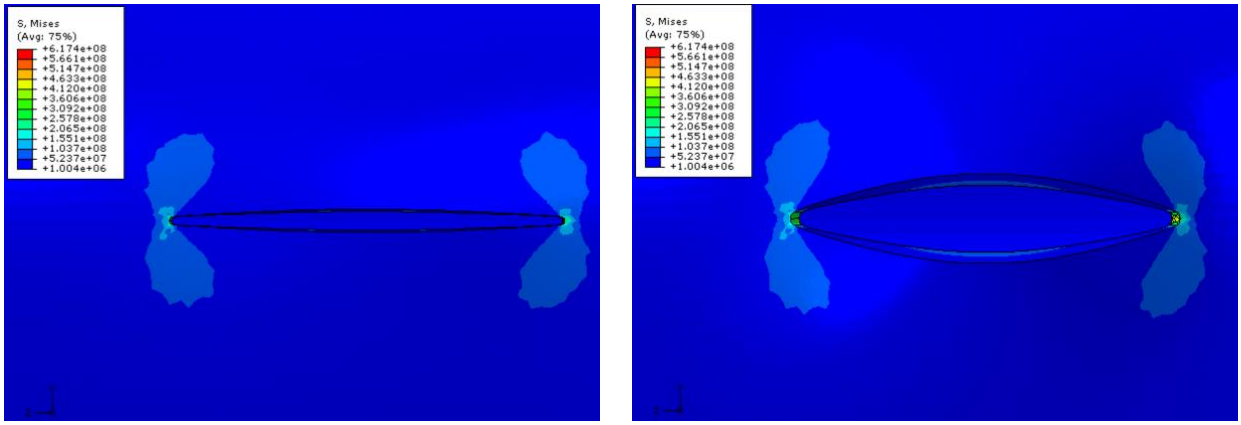

(a) (b)

Figure 3 – Stress distributions around a longitudinal crack using (a) normal and (b) deformed scales

Figure 4 shows the stress distribution around a spiral crack using fixed and deformed scales, while Figure 5 shows the same for a circumferential crack.

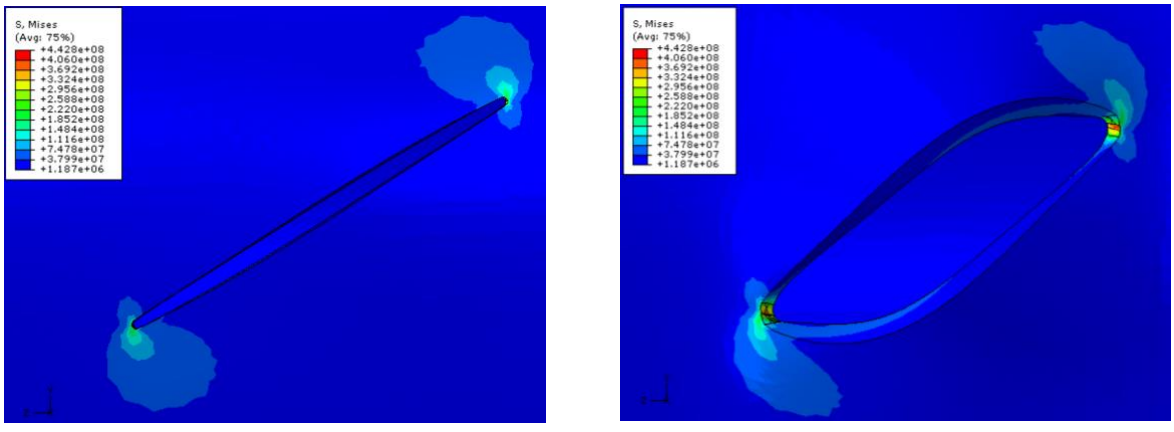

(a) (b)

Figure 4 – Stress distributions around a spiral crack using (a) normal and (b) deformed scales

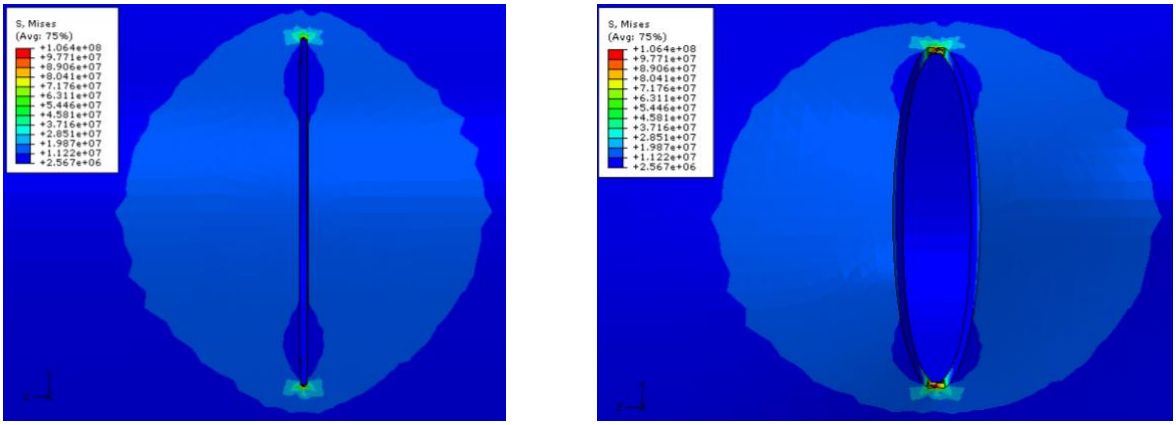

(a) (b)

Figure 5 – Stress distributions around a circumferential crack using (a) normal and (b) deformed scales

LEAK AREA AS A FUNCTION OF PRESSURE

The results of this and a previous study (Cassa et al. 2006) confirmed that the areas of leaks expand linearly with pressure, irrespective of the pipe material, leak type or loading state. This is also experimentally confirmed by others including Ferrante (2012). However, this is only true under linear elastic material behaviour and thus doesn't necessarily represent the behaviour of all leaks in a distribution system. In particular, Ferante et al (2012) and Massari et al (2011) showed that plastic pipe materials are subject to hysteresis, and thus do not adhere to the assumption of elastic behaviour. The results for a 60 mm longitudinal crack subject to different internal pressures are shown in Figure 6. This graph shows that the longitudinal crack expands outward with increasing pressure.

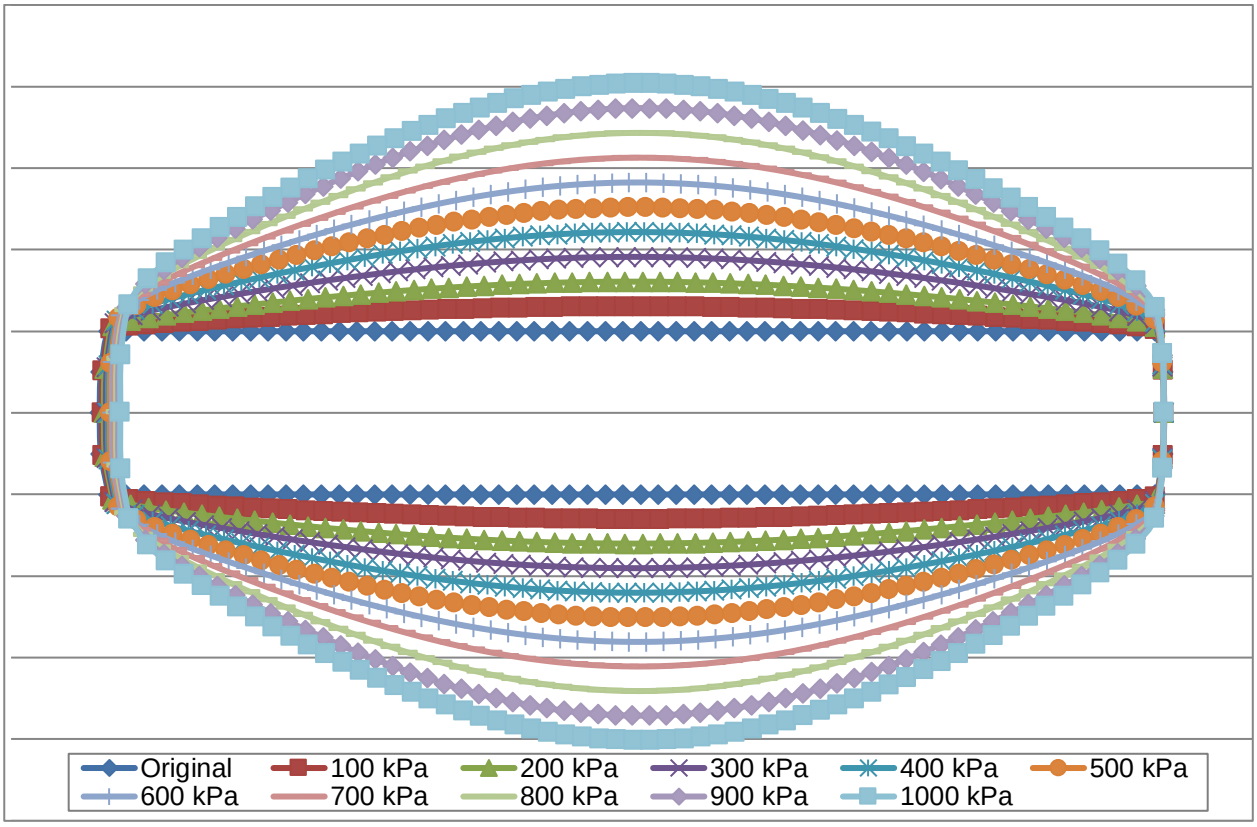

Figure 6 – 60 mm longitudinal crack at various pressures

The variations of leak area with pressure are shown in Figure 7 for 60 mm long longitudinal, circumferential and spiral cracks respectively as examples of the linear relationship found in all cases.

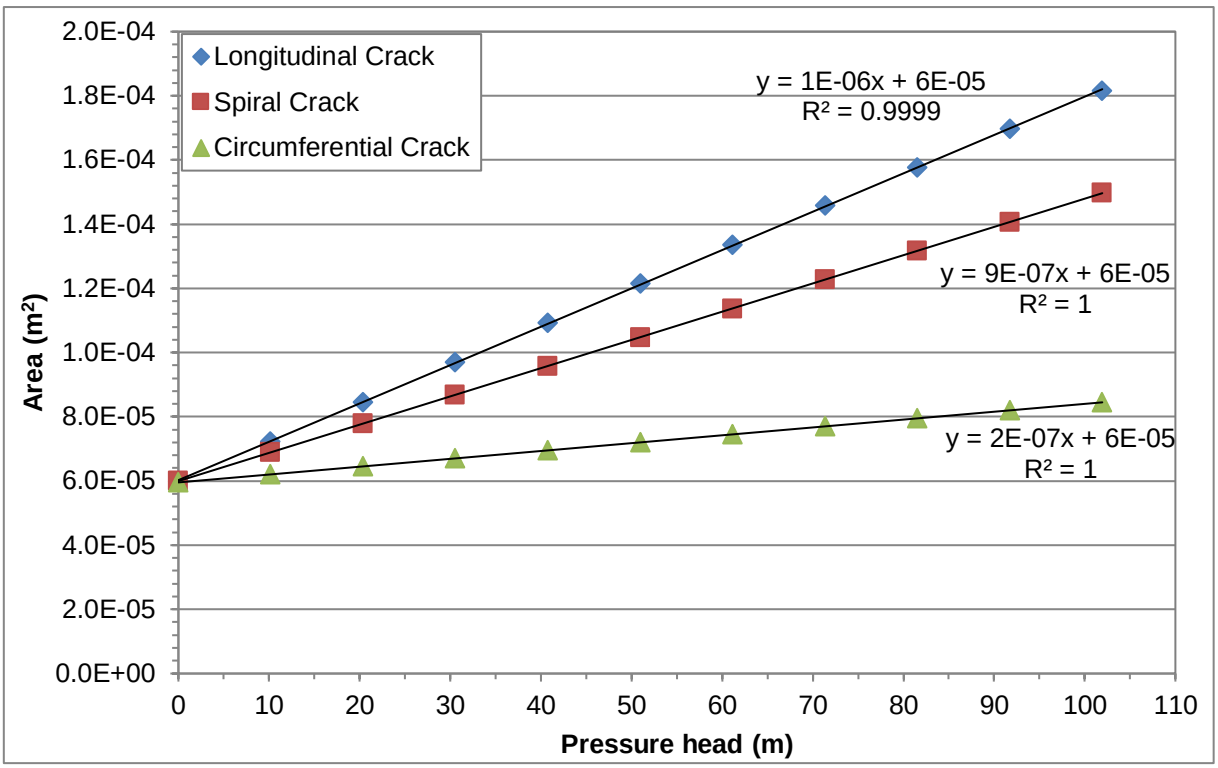

Figure 7 – Examples of the linear relationship between the area of a crack and the pressure head for longitudinal, circumferential and spiral cracks

This linear relationship has important implications for the modelling of leakage flows.

$$A = A_o + mh \tag{3}$$

Using this linear relationship in combination with the orifice equation, an expression for the leak flow can be found as a function of pressure:

$$Q = C_d\sqrt{2g}(A_o h^{0.5} + mh^{1.5}) \tag{4}$$

where Q is the flow in the orifice, C_d is the coefficient of discharge, g the gravitation constant, A_o the initial area of the orifice, h the pressure head and m the head-area slope. This equation is identical to that proposed by May (2004) and others, but is interpreted differently (Cassa et al. 2010): instead of interpreting leaks as either fixed or variable, all leaks are considered to have variable areas, although extent of variation differs for

different leaks. A leak can thus be characterised by its initial area (A_0) and its pressure-area slope *m*.

EFFECT OF PARAMETERS ON HEAD-LEAKAGE SLOPE *m*

Understanding what role each influencing parameter plays in the behaviour of the crack in relation to pressure is important when trying to predict a mathematical relationship describing this behaviour. Initially the base pipe of Table 1 was studied with only the pressure being varied to study the basic interaction between pressure and leakage and pressure and the leak area as shown in Figure 7. A sensitivity analysis was then conducted by varying each parameter in turn to study the effect of that parameter on the head-area slope of the pipe. Table 2 shows the values for the pipe and leak properties that were used in the sensitivity analysis, with the base pipe values shown in bold. The values were chosen to represent the typical range found in distribution system pipes in the field.

Table 2 – Variations in dimensions and properties of the pipe

Property or dimension	Varied
Pressure, P (kPa)	0, 100, 200, 300, 400, 500, **600**, 700, 800, 900, 1000
Young's modulus, E (GPa)	**3**, 10, 30, 90, 200
Poisson's ratio, v (-)	0.17, 0.21, 0.29, **0.4**, 0.45, 0.5
Longitudinal stress, σ_l (MPa) (excluding longitudinal cracks)	0, 1.3, 2.6, 3.9, **5.2**
Wall thickness, t (mm)	2, 2.5, **3**, 4, 5
Internal Diameter, ID (mm)	20, 30, 40, 50, 80, **104**, 150, 200, 250, 300, 350
Length of crack, L_{crack} (mm)	10, 30, **60**, 100, 130, 150
Width of crack, W_{crack} (mm)	0.1, 0.5, **1**, 2

Keeping all the parameters the same as the base pipe except the parameter being investigated, and varying each parameter in turn according to Table 2, the relationship between the head-area slope *m* and each parameter was obtained. It was also possible to

see which parameter affected the head-area slope the most. Figures 8 – 14 show how the head-area slope changes as the different parameters of the pipe are varied.

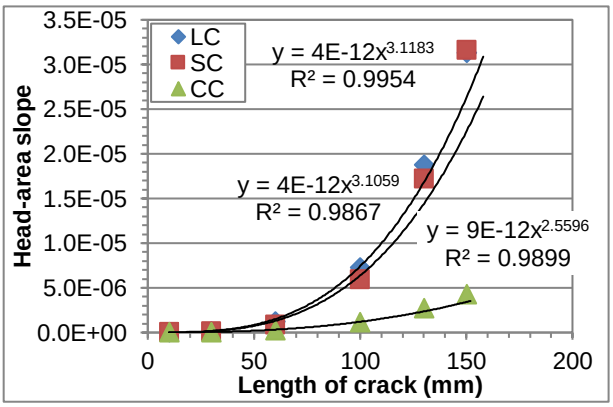

Figure 8 – Change in length of crack

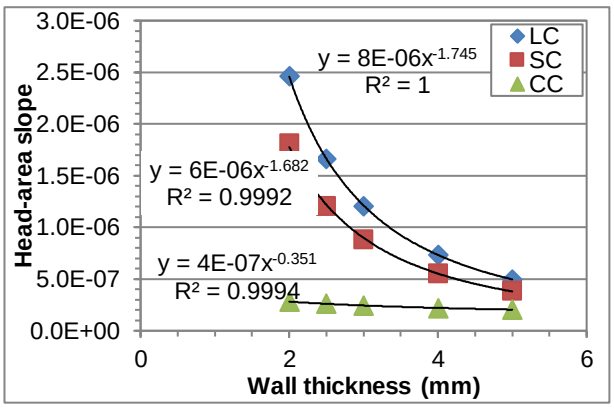

Figure 9 – Change in wall thickness

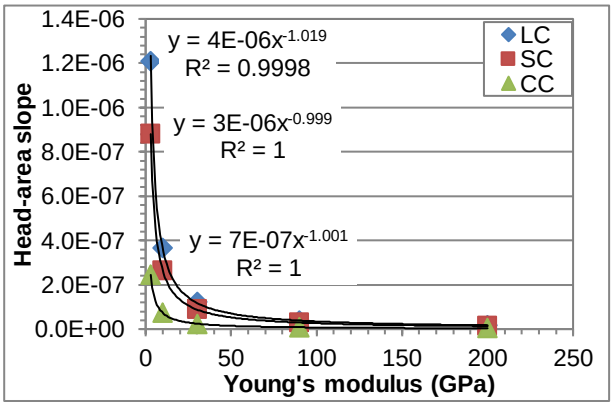

Figure 10 – Change in Young's modulus

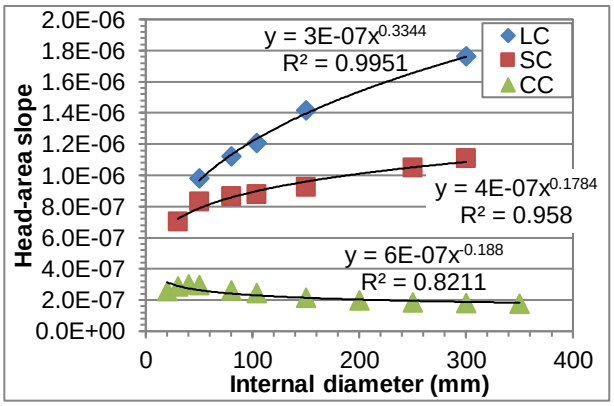

Figure 11 – Change in internal diameter

Results that can be gained from these graphs are the behaviour of the different parameters. In Figure 8 the length of crack shows head-area slope is proportional to the length of crack raised to the power of 3.12 for longitudinal cracks and a power of 3.11 for spiral cracks but a power of only 2.56 for circumferential cracks. In Figure 9 the head-area slope is inversely proportional to the wall thickness raised to a power of 1.75 for longitudinal cracks, a power of 1.68 for spiral cracks and only a power of 0.35 for circumferential cracks. In Figure 10 Young's modulus shows an inversely proportional relationship with the head-area slope for all three crack types. In Figure 11 the internal

diameter shows that the head-area slope is proportional to the internal diameter that is raised to the power 0.334 for longitudinal cracks and 0.178 for spiral cracks. For circumferential cracks however the behaviour is significantly different and could be attributed to the diameter-wall thickness ratio and the stiffness of the material.

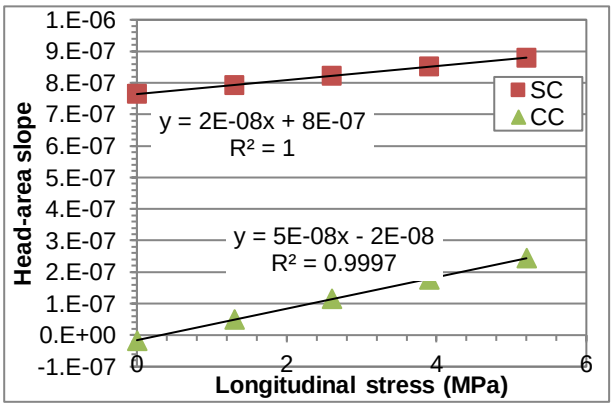

Figure 12 – Change in longitudinal stress

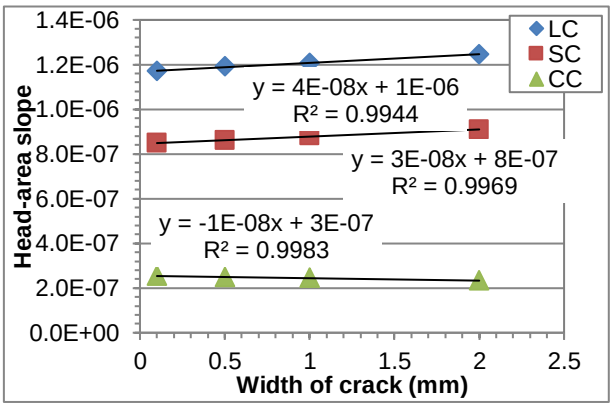

Figure 13 – Change in width of crack

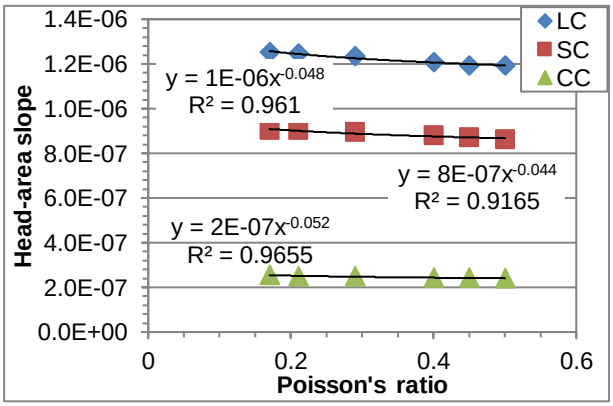

Figure 14 – Change in Poisson's ratio

In previous studies (Cassa et al. 2010) it was shown that the longitudinal stress has no effect of the behaviour longitudinal cracks. Thus Figure 12 shows only cracks orientated away from the longitudinal direction. The longitudinal stress has a small effect on the slope with spiral cracks but a larger effect with circumferential cracks, which gives a better understanding of the role of the material property of longitudinal stress in a pipe with cracks orientated away from the longitudinal. It is also noted that in absence of longitudinal stresses the circumferential crack has a negative pressure-area slope suggesting that the crack tries to close itself by expanding in the circumferential direction. Previous studies

done by the author and others confirm these findings with exponents lower than 0.5 observed in both numerical studies by Cassa et al. (2006) and experimental studies by Greyvenstein (2007). In Figure 13 the width of the crack shows a linear relationship with the head-area slope for all three crack types. From Figure 14 it can be seen that Poisson's ratio v has very little effect on the head-area slope *m*, which decreases as Poisson's ratio increases for all three cracks. This is evident in the small exponents of -0.048, -0.044 and -0.052 for longitudinal, spiral and circumferential cracks respectively.

Figure 15 shows a bar graph with all the parameters against the range over which the head-area slope *m* changes. Note that a logarithmic scale is used on the y-axis. As can be seen from the figure, the length of the crack has the dominant effect on the pressure-area slope for all three crack types followed by the wall thickness, Young's modulus and internal diameter. The relationship for the longitudinal stress show that these stresses have the lowest impact on longitudinal cracks, and the highest impact on circumferential cracks.

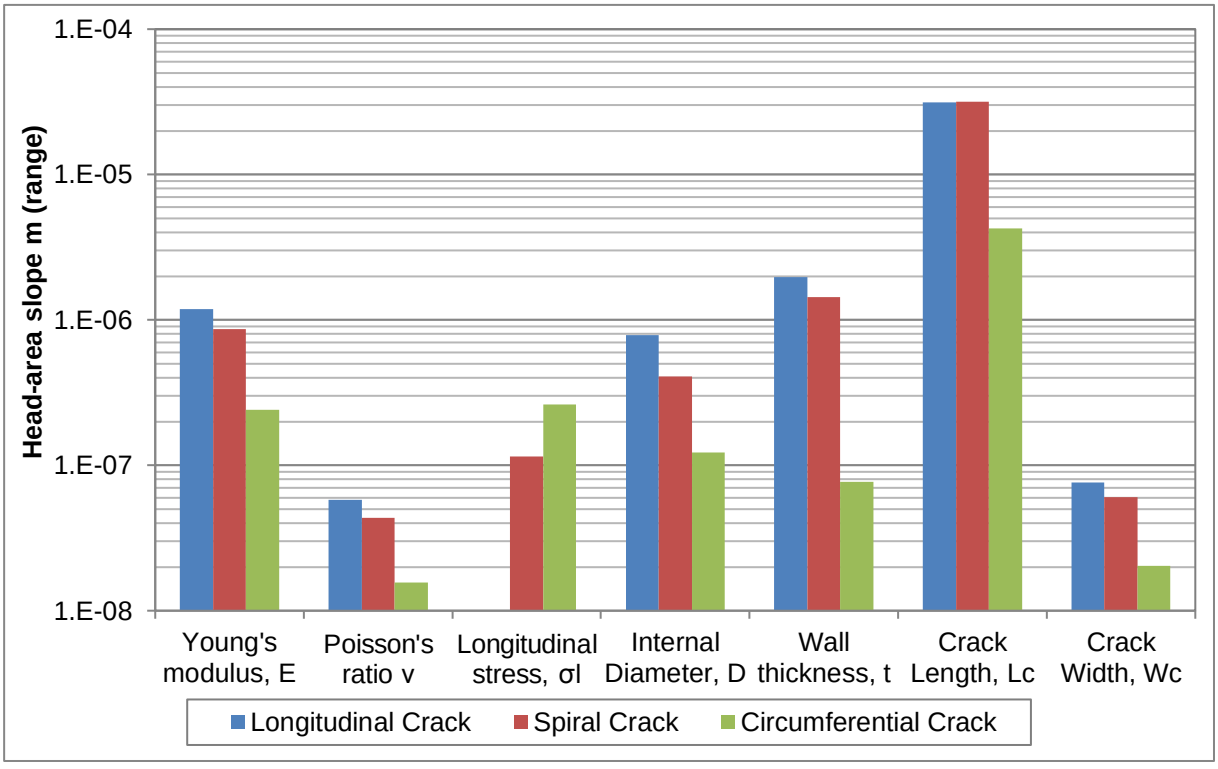

Figure 15 – Bar graph showing head-area slope range for each parameter

PREDICTING EQUATIONS FOR HEAD-AREA SLOPE *m*

Once all the relationships for all the parameters were obtained it was possible to use various data processing techniques to formulate mathematical relationships for the head-area slope as a function of the pipe and crack parameters. Regression analysis was used on the data to obtain three mathematical models describing the head-area slope *m* as a function of the parameters of the pipe and crack.

The three mathematical models obtained through regression analysis for longitudinal, spiral and circumferential crack respectively are:

$$\Delta A = 2.93157.\left(\frac{P}{E}\right).t^{-1.746}.d^{0.3379}.{L_c}^{4.80}.10^{0.5997(\log L_c)^2}$$

$$\Delta A = 3.7714.\left(\frac{P}{E}\right).t^{-1.6795}.d^{0.178569}.{L_c}^{6.051}.\sigma_l^{0.0928}.10^{1.05(\log L_c)^2} \quad (5)$$

$$\Delta A = 1.64802 \times 10^{-5}.\left(\frac{P}{E}\right).t^{-0.33824224}.d^{-0.186376316}.{L_c}^{4.87992662}.\sigma_l^{1.09182555}.10^{0.82763163(\log L_c)^2}$$

From Equation (5) it can be seen that the majority of the exponents are similar to those obtained in Figures 8 – 14 with the exception of the length of crack term. This is due to the fact that the crack length plays a large role in the behaviour of the pipe and needed a more sophisticated representation to adequately describe the pipe's response when various parameter are varied. It was found that the Poisson's ratio of the pipe material and width of the crack have negligible impact on the head-area slope, and thus are not included in the equations. The same is true for the longitudinal stress in the case of longitudinal cracks.

Using the linear relationship between pressure and leak area, Equation (4), these three models, Equation (5), give three equations for head-area slope from longitudinal, spiral and circumferential cracks

$$m = \frac{2.93157.d^{0.3379}.{L_c}^{4.80}.10^{0.5997(\log L_c)^2}.\rho.g}{E.t^{1.746}}$$

$$m = \frac{3.7714.d^{0.178569}.{L_c}^{6.051}.\sigma_l^{0.0928}.10^{1.05(\log L_c)^2}.\rho.g}{E.t^{1.6795}} \quad (6)$$

$$m = \frac{1.64802 \times 10^{-5}.{L_c}^{4.87992662}.\sigma_l^{1.09182555}.10^{0.82763163(\log L_c)^2}.\rho.g}{E.t^{0.33824224}.d^{0.186376316}}$$

Finally, using the proposed Equation (4) and Equations (6), three equations (7) for the cracks can be proposed for leakage out of an orifice:

$$Q = C_d\sqrt{2g}\left(A_0h^{0.5} + \frac{2.93157.d^{0.3379}.{L_c}^{4.80}.10^{0.5997(\log L_c)^2}.\rho.g}{E.t^{1.746}}h^{1.5}\right)$$

$$Q = C_d\sqrt{2g}\left(A_0h^{0.5} + \frac{3.7714.d^{0.178569}.{L_c}^{6.051}.\sigma_l^{0.0928}.10^{1.05(\log L_c)^2}.\rho.g}{E.t^{1.6795}}h^{1.5}\right) \quad (7)$$

$$Q = C_d\sqrt{2g}\left(A_0h^{0.5} + \frac{1.64802 \times 10^{-5}.{L_c}^{4.87992662}.\sigma_l^{1.09182555}.10^{0.82763163(\log L_c)^2}.\rho.g}{E.t^{0.33824224}.d^{0.186376316}}h^{1.5}\right)$$

Equations (7) can be used to predict the head-area slope *m* for any pipe section, material and crack length within the bounds of the regression analysis under the assumption of

linear elastic behaviour. The values of *m* predicted by the equations are compared to the finite element values in Figure 16 for all three cracks.

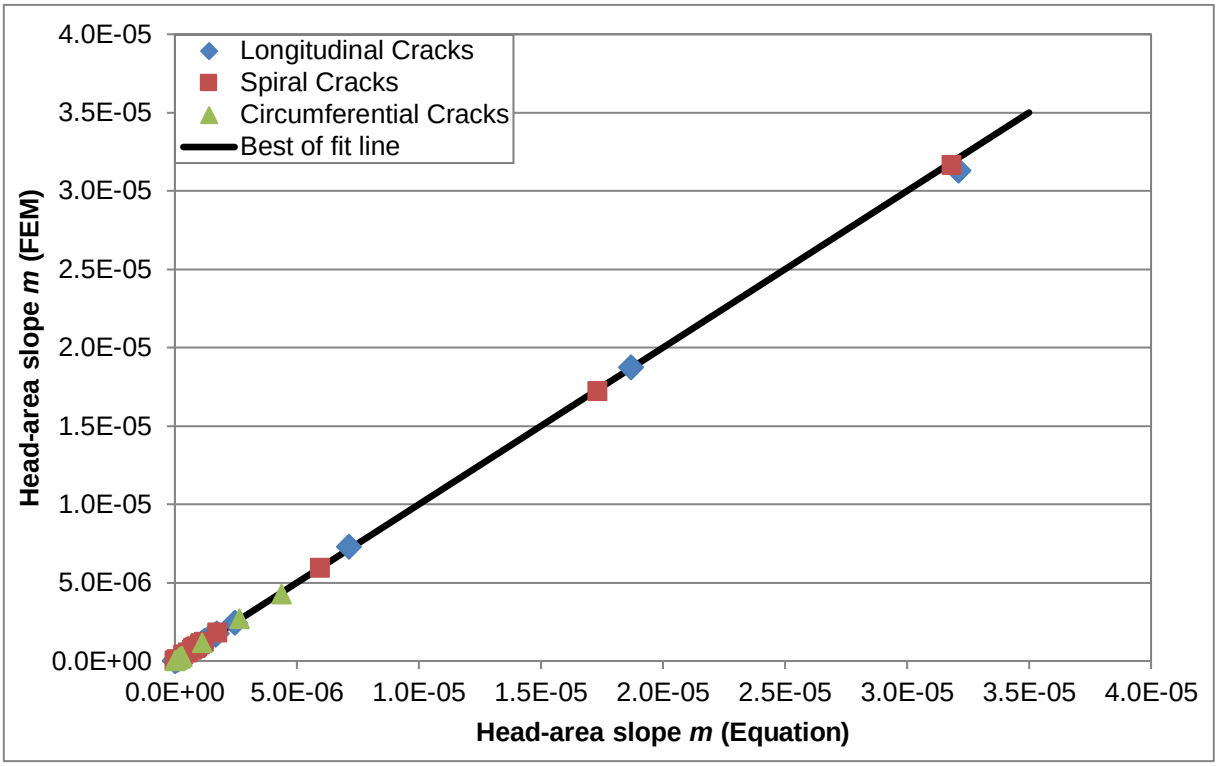

Figure 16 – Comparison of Equation (6) prediction of *m* to the finite element results for all three crack types

DISCUSSION AND CONCLUSION

The study investigated the effect of pressure on the leak area. This was done by increasing the internal pressure in the pipe and modelling the change in area of the crack. It showed that regardless of the orientation of the crack it was possible to express the leak area with a linear equation and then used it to propose a better description for leakage through an orifice.

This study also investigated the sensitivity of the head-area slope *m* to different material, section and crack properties. A realistic range values were determined for each parameter, after which the head-area slope was determined for this range. The investigation was repeated for longitudinal, circumferential and spiral cracks.

The main findings of the study are as follows:

- In general longitudinal cracks produced the highest head-area slopes, i.e. have the highest sensitivity to pressure, for equivalent parameter states followed by spiral and circumferential cracks.
- The only exception to this rule was the longitudinal pipe stress σ_l, which displayed the opposite behaviour. Longitudinal stresses had no effect on the sensitivity of longitudinal cracks, but the more the crack was orientated away from the longitudinal direction the greater the role played by the longitudinal pipe stress becomes.
- For the case where no longitudinal stresses are present in the pipe, it was found that the circumferential cracks can display leakage exponents below 0.5, and thus , meaning that the crack area is reducing with increasing pressure. This is due to the lengthening of the crack accompanied by a reduction in crack width due to the Poisson's ratio of the material. These results confirm earlier findings by Cassa et al. (2010) and Greyvenstein et al. (2007).
- The parameter that was found to have by the greatest impact on the head-area slope *m* was the crack length. This was followed by wall thickness, Young's modulus, internal diameter, longitudinal stress, crack width and Poisson's ratio. It was found that the impact of crack width and Poisson's ratio on the head-earea slope is small enough to be negligible.
- The relationship between the Young's modulus *E* and the head-area slope *m* was the same for all three crack types. It showed that the head-area slope was inversely proportional to the Young's modulus for all crack orientations.

- Three empirical equations were developed that may be used to predict the head-area slopes for the different cracks types. These equations are subject to the assumption of linear elastic behaviour, and thus may not be valid for cracks where plastic deformation or hysteresis occur. .

REFERENCES

Cassa, A. M., van Zyl, J. E. & Laubscher, R. F. 2006 A numerical investigation into the behaviour of leak openings in uPVC pipes under pressure. *Proc. WISA2006*, paper No. 438.

Cassa, A. M., van Zyl, J. E. & Laubscher, R. F. 2010 A Numerical investigation into the effect of pressure on holes and cracks in water supply pipes. *Urban Water Journal* **7** (2) 109-121.

Chadwick, A. & Morfett, J. 1999 *Hydraulics in Civil and Environmental Engineering*. 3rd ed. E & FN Spon, London.

Farley, M. & Trow, S. 2003 *Losses in Water Distribution Networks.* IWA Publishing, London.

Ferrante, M. 2012 Experimental Investigation of the Effects of Pipe Material on the Leak Head-Discharge Relationship. *Journal of Hydraulic Engineering* ASCE **138** (8) 736-743. doi:10.1061/(ASCE)HY.1943-7900.0000578

Ferrante, M., Massari, C., Brunone, B., & Meniconi, S. 2011 Experimental Evidence of Hysteresis in the Head-Discharge Relationship for a Leak in a Polyethylene Pipe. *Journal of Hydraulic Engineering* ASCE **137** 775-780. doi:10.1061/(ASCE)HY.1943-7900.0000360

Massari, C., Ferrante, M., Brunone, B., & Meniconi, S. 2012 Is the leak head-discharge relationship in polyethylene pipes a bijective function? *Journal of Hydraulic Research* IAHR **50**(4) 409-417. doi:10.1080/00221686.2012.696558

Gere, J. M. 2001 *Mechanics of Materials*. 5th ed. Brooks/Cole, United States.

Greyvenstein, B., van Zyl, JE 2007 An experimental investigation into the pressure-leakage relationship of some failed water pipes. *Journal of Water Supply-AQUA* **56** (2) 117-124.

Huebner, K. H. et al. 2001 *The Finite Element Method for Engineers.* 4th ed. John Wiley & Sons, Inc., New York.

May, J. (October 2004) *Pressure Dependent Leakage.* World Water and Environmental Engineering.